# Neural modelling of compactibility characteristics of cohesionless soil

Maria J. Sulewska

*Faculty of Civil and Environmental Engineering, Bialystok University of Technology*
*ul. Wiejska 45A, 15-351 Białystok, Poland*
*e-mail: m.sulewska@pb.edu.pl*

Compaction is the method of in-situ soil modification to improve its engineering properties. Two key compactibility parameters are: the maximum dry density $\rho_{\mathrm{d\,max}}$ and the corresponding optimum water content $w_{\mathrm{opt}}$. They are basic parameters for designing, constructing and controlling the compaction quality of earth structures (e.g. earth dams, highway embankments). Soil compactibility can be determined from the laboratory compactibility curve basing on Proctor's test. However, this test is destructive, time-consuming and expensive. To facilitate the determination of the cohesionless soil compactibility parameters, correlations between $\rho_{\mathrm{d\,max}}$ and $w_{\mathrm{opt}}$ and the basic parameters characterizing soil grain-size distribution ($C_{\mathrm{U}}$, $D_{10}$, $D_{20}$, $D_{30}$, $D_{40}$, $D_{50}$, $D_{60}$, $D_{70}$, $D_{80}$, and $D_{90}$) were developed. Artificial neural networks are applied to determine models with good prediction quality. The neural models have higher accuracy than the classic statistical models.

**Keywords:** Geotechnical engineering, cohesionless soil, compactibility characteristics, Artificial Neural Network

## 1. INTRODUCTION

Compaction is an efficient method for improving subsoil and soil materials in earth structures. The purpose of soil compaction is to decrease the soil porosity, deformability and water permeability, and also to increase its load-bearing capacity. Soil can be compacted by static (kneading with static rollers or tyre rollers) or dynamic methods (vibration rollers, heavy ramming or explosions). The degree of compaction, $D$ (or relative compaction, $C_{\mathrm{r}}$) is used for checking-up the compaction of cohesive and cohesionless soils in compacted and erected embankments [1, 2]. It is defined as the following ratio:

$$D = \frac{\rho_{\mathrm{d}}}{\rho_{\mathrm{d\,max}}},$$

(1)

where $\rho_{\mathrm{d}}$ is the dry density of solid particles in embankment $(\mathrm{Mg/m^3})$ and $\rho_{\mathrm{d\,max}}$ $(\mathrm{Mg/m^3})$ is the maximum dry density tested by Proctor's method [3–5]. However, density index, $I_{\mathrm{D}}$ (or relative density $D_{\mathrm{R}}$) is used for estimation of compaction of cohesionless soils built in ground, naturally compacted as a result of geological process [5, 6].

## 2. PARAMETERS OF SOIL COMPACTIBILITY

Compactibility describes the ability of soil to reach certain values of $\rho_{\mathrm{d}}$. This dry soil density depends on the energy used and its transfer to the soil for compaction, the type of soil and the soil moisture at compaction. Two key compactibility parameters are: the maximum dry density $\rho_{\mathrm{d\,max}}$ and the corresponding optimum water content $w_{\mathrm{opt}}$. They define the optimal compaction

point. Compactibility depends on physical soil properties: grain and lithology compositions, grain shape and soil origin. The $\rho_{d\,max}$ and $w_{opt}$ can only be determined experimentally, using Proctor's method from the compaction curve (i.e. density moisture relationship) [3, 4]. There was developed a standard Proctor's method in this study. Proctor's test is laborious, time-consuming and leads to significant delays in construction; therefore simpler methods of testing the compaction parameters are needed.

The purpose of this research is to analyze the influence of soil grain-size distribution on its compactibility, and to determine the relationship between parameters characterizing grain-size distribution of granular (cohesionless) soils and their compactibility parameters.

## 3. GRAIN-SIZE DISTRIBUTION

Grain-size distribution is defined by the following parameters: uniformity coefficient $C_U$, curvature coefficient $C_C$, and grain diameters $D_x$ (mm), below which $x\%$ of soil mass is placed, for $x = 10$, 20, 30, 40, 50, 60, 70, 80 and 90. Parameters $C_U$ and $C_C$ are defined as the following ratios:

$$C_U = \frac{D_{60}}{D_{10}}, \tag{2}$$

$$C_C = \frac{D_{30}^2}{D_{10}D_{60}}. \tag{3}$$

Two methods of testing grain-size distribution were used: sieve analysis for gravels and sands with grains $> 0.071\,\text{mm}$, or aerometric analysis for cohesive soils and silty sands with grains $< 0.071\,\text{mm}$.

## 4. INFLUENCE OF GRAIN-SIZE DISTRIBUTION ON COMPACTIBILITY OF COHESIONLESS SOILS

Dependence models of compaction parameters have been in use for many years. Empirical models to predict optimum compaction characteristics of fine-grained (cohesion) soils in relation to their properties and the compaction energy, were constructed for cohesive soils. There are statistical correlations [7–9] and models basing on artificial neural networks for estimating of the Proctor's parameters $\rho_{d\,max}$ and $w_{opt}$ [10, 11]. There are studies, which modelled the compaction curves rather than only the compaction characteristics, too [12].

The uniformity coefficient $C_U$ significantly influences the compactibility of cohesionless soil [13]; the higher is the $C_U$ value, the higher will be the $\rho_{d\,max}$ and the lower – the $w_{opt}$. Soil grain-size distribution has significant influence on the compactibility parameters, see [3].

## 5. EXPERIMENTAL METHOD

Laboratory tests were conducted for cohesionless soils. The origin of soils was post-glacial, from northeast Poland. Range of examinations is shown in Fig. 1. Compactibility characteristics and grain-size distribution parameters for 121 soils from six tested groups were analyzed. Soils from the following groups were tested: silty sand (21 samples), fine sand (47 samples), medium sand (24 samples), coarse sand (13 samples), sand and gravel mix (11 samples), and gravel (5 samples). All soils were compacted using the standard Proctor method [3, 4]. The examples of grain-size distribution curves of tested soils are given in Fig. 2. The values of analyzed geotechnical parameters are given in Table 1.

**Table 1.** The analyzed geotechnical parameters of tested soils

| Type of soil | Silty sand | Fine sand | Medium sand | Coarse sand | Sand and gravel mix | Gravel | Total |
|---|---|---|---|---|---|---|---|
| Soil code | 1 | 2 | 3 | 4 | 5 | 6 | 1–6 |
| Number of pattern | 21 | 47 | 24 | 13 | 11 | 5 | 121 |
| $w_{opt}$ [%] | 9.9–16.6 | 10.5–17.7 | 6.9–13.5 | 4.3–12.8 | 5.9–8.7 | 2.1–6.9 | 2.1–17.7 |
| $\rho_{d\,max}$ [Mg/cm³] | 1.607–1.800 | 1.587–1.880 | 1.640–2.004 | 1.800–1.942 | 1.840–2.120 | 2.130–2.200 | 1.587–2.200 |
| $C_U$ | 1.80–4.75 | 1.25–2.53 | 1.26–4.57 | 3.32–7.52 | 2.90–12.50 | 7.38–10.26 | 1.25–12.50 |
| $C_C$ | 0.70–2.15 | 0.71–1.95 | 0.74–1.53 | 0.49–1.33 | 0.56–1.21 | 0.98–3.10 | 0.49–3.10 |
| $D_{10}$ [mm] | 0.019–0.125 | 0.080–0.170 | 0.140–0.360 | 0.170–0.250 | 0.165–0.540 | 0.390–0.500 | 0.019–0.500 |
| $D_{20}$ [mm] | 0.040–0.170 | 0.100–0.215 | 0.180–0.430 | 0.195–0.420 | 0.250–0.830 | 0.740–1.000 | 0.040–1.00 |
| $D_{30}$ [mm] | 0.040–0.200 | 0.120–0.240 | 0.200–0.450 | 0.280–0.500 | 0.360–1.200 | 1.150–2.200 | 0.040–2.20 |
| $D_{40}$ [mm] | 0.060–0.215 | 0.120–0.250 | 0.220–0.470 | 0.340–0.930 | 0.500–1.600 | 2.000–2.850 | 0.060–2.85 |
| $D_{50}$ [mm] | 0.074–0.220 | 0.120–0.260 | 0.250–0.800 | 0.420–1.300 | 0.630–2.350 | 2.450–3.500 | 0.070–3.50 |
| $D_{60}$ [mm] | 0.084–0.250 | 0.125–0.300 | 0.260–0.660 | 0.630–1.730 | 0.830–3.750 | 2.950–4.500 | 0.084–4.500 |
| $D_{70}$ [mm] | 0.093–0.300 | 0.128–0.320 | 0.260–0.850 | 0.860–1.700 | 1.150–6.000 | 3.650–5.900 | 0.093–6.000 |
| $D_{80}$ [mm] | 0.110–0.395 | 0.135–0.450 | 0.270–1.200 | 1.150–2.500 | 1.700–10.00 | 4.900–9.000 | 0.110–10.00 |
| $D_{90}$ [mm] | 0.140–0.400 | 0.150–0.850 | 0.320–1.850 | 1.500–5.000 | 2.350–25.00 | 8.000–17.50 | 0.140–25.00 |

**Table 3.** Accuracy statistics of the best ANN models

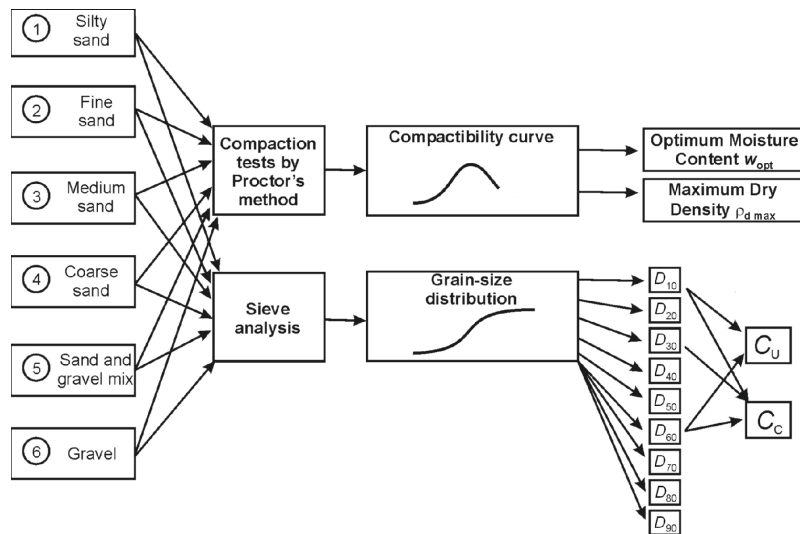| Model | Outputs | Inputs | Best topology | RSME | | | $R^2$ | | | Epoch number |
|---|---|---|---|---|---|---|---|---|---|---|
| | | | | L | V | T | L | V | T | |
| 1 | $w_{opt}$ | $C_U, D_{10}, D_{20}, D_{70}, D_{80}$ | 5-4-1 | 0.121 | 0.122 | 0.159 | 0.75 | 0.76 | 0.65 | 940 |
| 2 | $\rho_{d\,max}$ | $C_U, D_{10}, D_{20}, D_{30}, D_{40}, D_{50}, D_{60}, D_{70}, D_{80}, D_{90}$ | 10-4-1 | 0.077 | 0.080 | 0.085 | 0.91 | 0.91 | 0.89 | 172 |
| 3 | $w_{opt}$ $\rho_{d\,max}$ | $C_U, D_{20}, D_{30}, D_{40}, D_{50}, D_{60}, D_{80}, D_{90}$ | 8-9-2 | 0.107 | 0.115 | 0.109 | 0.72 0.90 | 0.71 0.90 | 0.73 0.89 | 65 |

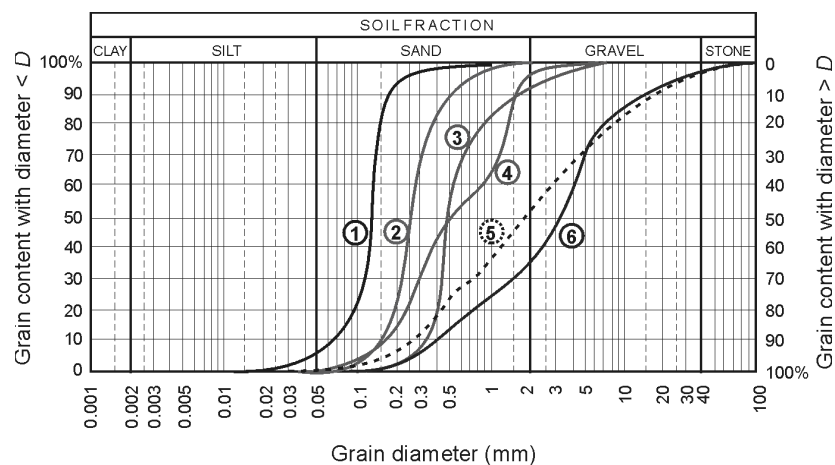**Fig. 1.** Range of laboratory tests



**Fig. 2.** Grain-size distribution curves of selected tested soils from groups 1–6

## 6. Statistical analysis of tests results

The compactibility parameters $\rho_{d\,max}$ and $w_{opt}$ were tested for dependence on the soil type (i.e. grain-size distribution) by statistical analysis, using linear simple and multiple regressions. The statistical analysis, discussed in the presented paper, was performed using the STATISTICA computer system [14].

### 6.1. Influence of soil type upon geotechnical parameters

Testing of difference significance [15, 16] for soil groups was carried out to determine whether compactibility parameters are dependent on the soil type. The following steps were performed: (i) $\rho_{d\,max}$ and $w_{opt}$ were divided into six subsets, depending on soil type, (ii) fitting of analyzed variables to a normal distribution, in the whole data set and in six subsets, using tests of normality (Kolmogorov-Smirnow and W Shapiro-Wilk) and nonparametric tests of goodness-of-fit (Kolmogorov-Smirnow)

at the significance level $\alpha = 0.05$. The $\rho_{d\,max}$ and $w_{opt}$ were normally distributed neither over the entire data nor in most data subsets, ($iii$) nonparametric test of significance (Kruskal-Wallis) was used to check the null hypothesis, that separated subsets from the same population. The result indicated that soil type (i.e. grain-size distribution) had a statistically significant effect on average of $\rho_{d\,max}$ and $w_{opt}$, as depicted in Figs. 3 and 4, where the average value, $\bar{y}$, and standard deviation, $s$, are expressed as

$$\bar{y} = \frac{1}{N} \sum_{i=1}^{N} y_i,$$ (4)

$$s = \sqrt{\frac{1}{N} (y_i - \bar{y})^2},$$ (5)

where $y_i$ are the measured values and $N$ is the number of pattern.
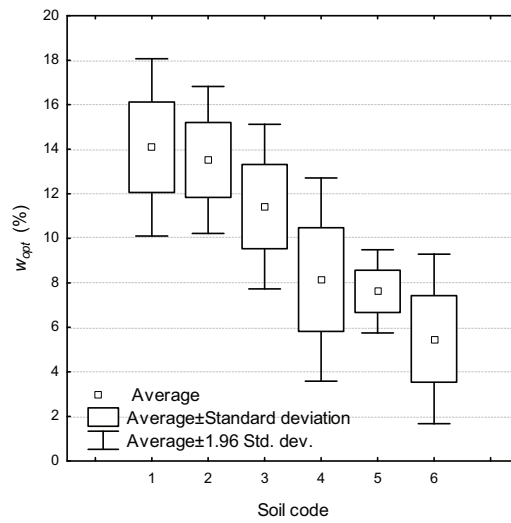


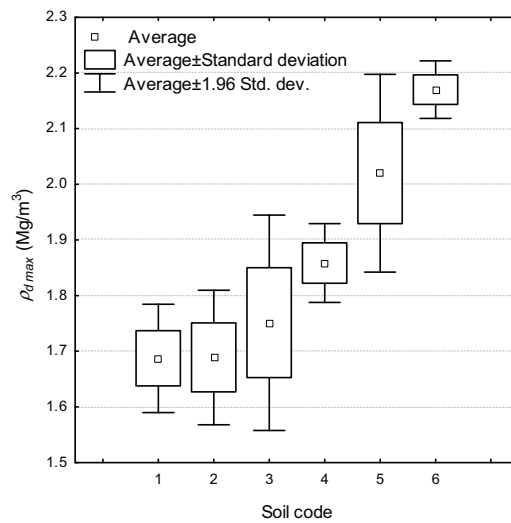**Fig. 3.** Average values of $w_{opt}$ for groups of soils 1–6



**Fig. 4.** Average values of $\rho_{d\,max}$ for groups of soils 1–6

## 6.2. Simple correlations

The matrix of correlation coefficients $r$ is shown in Table 2. These coefficients allow to analyze the relationships between the variables [17–19]. The more the correlation coefficient is close to value 1,

**Table 2.** Matrix of correlation coefficients $r$, between the compactibility parameters and the grain size parameters

| Variable | $w_{\text{opt}}$ | $\rho_{\text{d max}}$ | $C_{\text{U}}$ | $C_{\text{C}}$ | $D_{10}$ | $D_{20}$ | $D_{30}$ | $D_{40}$ | $D_{50}$ | $D_{60}$ | $D_{70}$ | $D_{80}$ | $D_{90}$ |
|---|---|---|---|---|---|---|---|---|---|---|---|---|---|
| $w_{\text{opt}}$ | 1.00 | | | | | | | | | | | | |
| $\rho_{\text{d max}}$ | -0.82 | 1.00 | | | | | | | | | | | |
| $C_{\text{U}}$ | -0.68 | 0.85 | 1.00 | | | | | | | | | | |
| $C_{\text{C}}$ | 0.26 | -0.25 | -0.21 | 1.00 | | | | | | | | | |
| $D_{10}$ | -0.67 | 0.73 | 0.55 | -0.21 | 1.00 | | | | | | | | |
| $D_{20}$ | -0.70 | 0.79 | 0.66 | -0.01 | 0.94 | 1.00 | | | | | | | |
| $D_{30}$ | -0.69 | 0.80 | 0.78 | 0.11 | 0.86 | 0.97 | 1.00 | | | | | | |
| $D_{40}$ | -0.68 | 0.82 | 0.79 | 0.05 | 0.84 | 0.95 | 0.99 | 1.00 | | | | | |
| $D_{50}$ | -0.69 | 0.84 | 0.84 | -0.02 | 0.83 | 0.93 | 0.96 | 0.99 | 1.00 | | | | |
| $D_{60}$ | -0.71 | 0.87 | 0.88 | -0.10 | 0.81 | 0.89 | 0.93 | 0.97 | 0.99 | 1.00 | | | |
| $D_{70}$ | -0.71 | 0.87 | 0.90 | -0.16 | 0.78 | 0.84 | 0.88 | 0.92 | 0.95 | 0.98 | 1.00 | | |
| $D_{80}$ | -0.67 | 0.84 | 0.86 | -0.20 | 0.74 | 0.77 | 0.80 | 0.85 | 0.89 | 0.93 | 0.98 | 1.00 | |
| $D_{90}$ | -0.56 | 0.73 | 0.69 | -0.14 | 0.62 | 0.65 | 0.68 | 0.69 | 0.72 | 0.75 | 0.82 | 0.88 | 1.00 |

the stronger will be the linear correlation between the tested variables. Correlations between the variables are calculated by means of formula

$$r = \frac{\sum\limits_{i=1}^{N} (x_i - \bar{x})(y_i - \bar{y})}{\sqrt{\sum\limits_{i=1}^{N} (x_i - \bar{x})^2 \sum\limits_{i=1}^{N} (y_i - \bar{y})^2}},$$ (6)

where $\bar{x}$, $\bar{y}$ are the averages of the $x_i$ and $y_i$ values. The obtained matrix of correlation coefficients indicate that:

(i) there are statistically significant simple correlations between compactibility parameters ($\rho_{\text{d max}}$ and $w_{\text{opt}}$) and granulation parameters ($C_{\text{U}}$, $D_{10}$, $D_{20}$, $D_{30}$, $D_{40}$, $D_{50}$, $D_{60}$, $D_{70}$, $D_{80}$, and $D_{90}$). All diameters $D_x$ similarly influence the compactibility parameters and none of them is clearly different,

(ii) there are negative correlations between $w_{\text{opt}}$ and $D_x$, and positive correlations between $\rho_{\text{d max}}$ and $D_x$,

(iii) $C_{\text{C}}$ has weak correlations with compactibility and with granulation parameters. This indicates that $C_{\text{C}}$ does not contain any important soil information and consequently, will be not further analyzed,

(iv) $C_{\text{U}}$ significantly influences $w_{\text{opt}}$ and $\rho_{\text{d max}}$. Linear dependences and best non-linear dependences [17–20] are presented in Figs. 5 and 6.

The coefficient of determination $R^2$ applied as a criterion of the model evaluation

$$R^2 = 1 - \frac{\sum\limits_{i=1}^{N} \left(y_i - \widehat{y}_i\right)^2}{\sum\limits_{i=1}^{N} (y_i - \bar{y})^2},$$ (7)
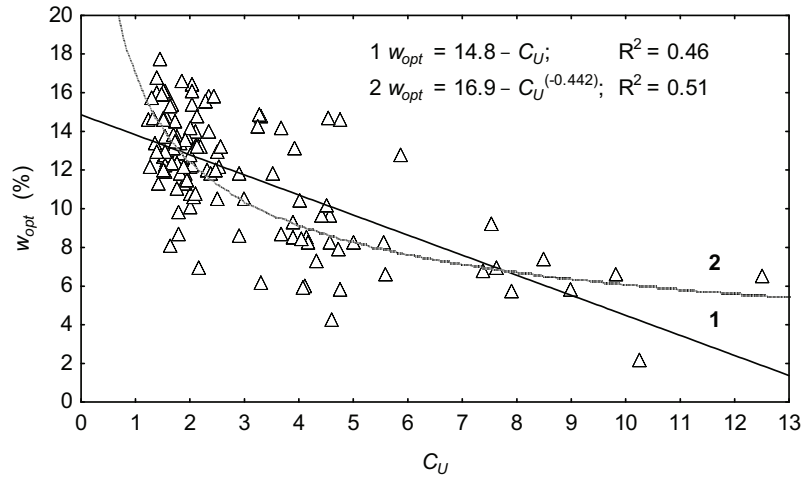
**Fig. 5.** Relationships $w_{\text{opt}} = f(C_{\text{U}})$
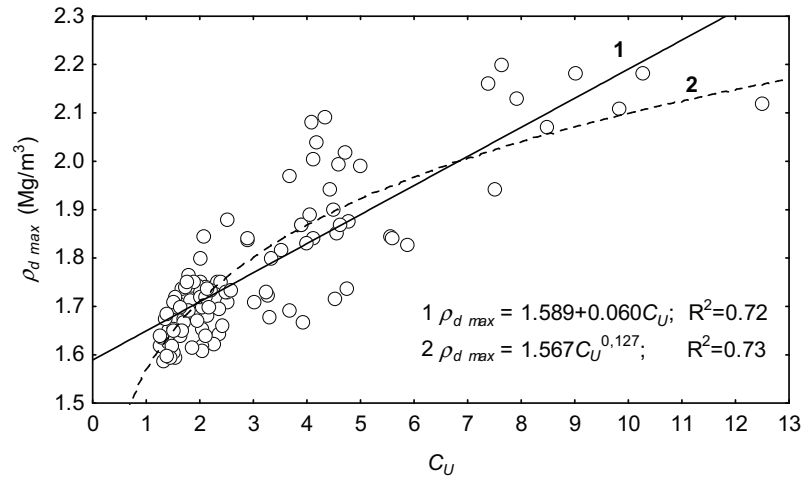


**Fig. 6.** Relationships $\rho_{\text{d max}} = f(C_{\text{U}})$

where $y_i$ is the actual value, $\widehat{y}_i$ is the predicted value of $y$, and $\bar{y}$ is the mean of the $y_i$ values. A perfect fitting corresponds to $R^2$ equal 1, a good fitting is near 1, and a poor fitting is near 0.

## 6.3. Multiple correlation models

Multiple linear regressions [17] were then carried out, where the applied variables were all grain-size distribution parameters:

$$
\begin{aligned}
w_{\text{opt}} = {}& 17.7 - 1.2C_{\text{U}} - 18.3D_{10} - 1.6D_{20} - 2.9D_{30} - 4.7D_{40} \\
& + 9.2D_{50} - 0.3D_{60} - 2.0D_{70} + D_{80} - 0.1D_{90},
\end{aligned}
\tag{8}
$$

$$
\begin{aligned}
\rho_{\text{d max}} = {}& 1.518 + 0.054C_{\text{U}} + 0.445D_{10} + 0.259D_{20} - 0.112D_{30} + 0.317D_{40} \\
& - 0.386D_{50} + 0.109D_{60} - 0.021D_{70} - 0.003D_{80} + 0.005D_{90}.
\end{aligned}
\tag{9}
$$

The multiple linear regression relation (8) has $R^2 = 0.64$. Only $C_{\text{U}}$ and $D_{10}$ are statistically significant, other variables are not. The model (9) has better predictive value with $R^2 = 0.85$. Only

$C_U$ and $D_{50}$ are statistically significant in this multiple regression model, too. Comparison between the tested $w_{opt}$ values, those values predicted by Eq. (8), as well as tested $\rho_{d\,max}$ values and those predicted from Eq. (9), are presented in Figs. 7 and 8. The relative errors calculated by the formula (10) are used in Figs. 7 and 8. The values of $w_{opt}$ are predicted basing on Eq. (8) with relative error about 35%, and the relative error of $\rho_{d\,max}$ prediction related to Eq. (9) is about 10%.

$$RE = \left| \frac{\widehat{y}_i - y_i}{\widehat{y}_i} \right| \cdot 100\%. \tag{10}$$
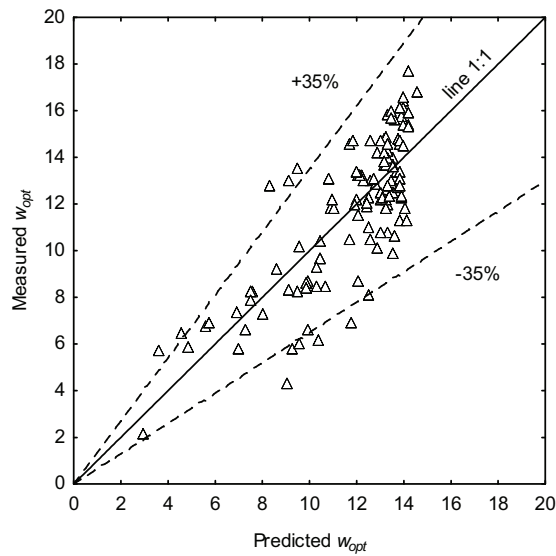


**Fig. 7.** Comparison between the tested $w_{opt}$ values and predicted values from Eq. (8), with $\pm 35\%$ $RE$ line
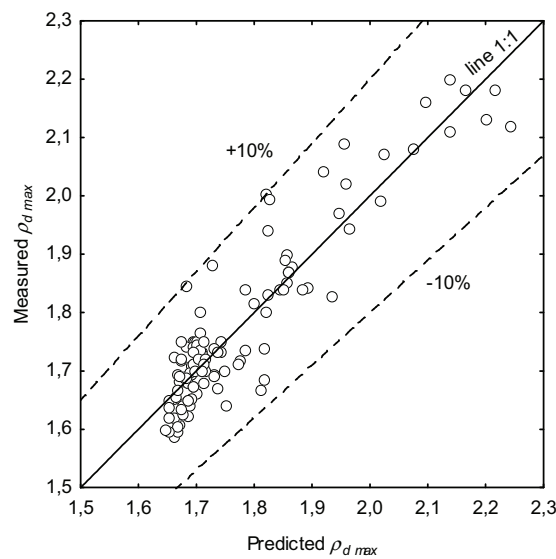


**Fig. 8.** Comparison between the tested $\rho_{d\,max}$ values and predicted values from Eq. (9), with $\pm 10\%$ $RE$ line

## 7. Some remarks on artificial neural networks

Artificial neural networks (ANNs) are calculated using the principle of simultaneous work of individual neurons. Artificial neurons act as specific converters of signals [21–23]. The neuron body is composed of two boxes: summing junction $\Sigma$ and activation (threshold) unit $F$. In the AN model, the following variables and parameters are used: $\boldsymbol{x} = \{x_1, \ldots, x_j, \ldots, x_N\}$ is input vector, $\boldsymbol{w} = \{w_1, \ldots, w_j, \ldots, w_N\}$ is vector of synaptic weights, $N$ is the number of input variables, $b = -\theta = w_0$ is bias (threshold parameter), $F(\nu)$ is the activation function of neuron, $\nu = u + b = \sum_{j=1}^{N} w_j x_j - \theta$ is the potential of neural network.

Work of the neurons in the network can be described in the following way. Every input $x_i$ is connected with weight $w_i$, by which the input signal is multiplied. Signal is transferred in the form: amplified (when $w_i > 1$), reduced (when $w_i < 1$), opposite to signals from other inputs (when $w_i < 0$), and a lack of connection between neurons (when $w_i = 0$). After multiplying by weights, the signals are summed up in a neuron. From this sum, the threshold value is deducted. The sum of signals processed in this way is the total stimulation of neuron. The signal of the total neuron stimulation is then transformed by the activation function into an output signal. Activation functions can be of scalar product or radial function forms. They are most frequently in the form of identity, sigmoid (logistic or binary sigmoid) or bipolar sigmoid functions.

ANNs significantly extend the application of traditional regression modelling, due to their approximation abilities [24]. Regression problems can be solved using the following neural networks: linear networks, multi-layer perceptrons (MLP), radial basis functions, generalized regressional neural networks [21–25] . MLP has been applied in the present study. MLPs are feed-forward networks, where signals flow from input to output. The neural analysis was performed by using the STATISTICA Neural Networks computer program [26].

The process of constructing MLP networks consists of several stages. Stage 1 is a selection of representative set of training data (input and output signals), which may fully represent the solved issue. The ANN is trained on examples, thus creating a model composed of a certain number of cases, described by input and the respective output values. The whole set of cases is divided (most commonly at random) into three subsets: learning ($L$), validating ($L$) and testing ($T$). For this study, 50% ($L = 61$) of the original data patterns were extracted at random to train the neural networks. The remaining 50% of the data patterns were used as follows: 25% for the validation subset ($V = 30$) and 25% for the testing subset ($T = 30$).

Stage 2 is the selection of the network architecture. The number of hidden layers, the number of neurons in particular hidden layers and the activation function used in neurons of hidden and output layers, should be defined to select the architecture of MLP neural network. The number of input neurons (usually equal to the number of independent variables) and output neurons (usually one neuron) are determined by the type of problem. Determination of the number of hidden layers (usually 1–2) and the number of neurons in these layers is empirical. Three-layer neural networks with input layer, hidden layer and output layer, were applied in the present study. For the ANN models developed in this study, a bipolar sigmoid activation function was used for the hidden layer neurons.

Stage 3 is an automatic process of network training. The aim of the training is determination of the weighting, which gives output values closest to the observed values of the dependent variable. The training process is stochastic, since its course and final result are not precisely determined. Training algorithms have an iterative character, within each iteration (i.e. epoch) all cases of the learning set are presented to the ANN.

The most effective method was the Variable Metric Method with algorithm of the Broyden-Fletcher-Goldfarb-Shanno (BFGS) in this study [27, 28]. A $V$ set controls the training progress. During training there is a simultaneous decrease of error for $L$ and $V$ sets. The iteration process is stopped when validation error begins to increase, which indicates 'overfitting' and that the network is losing ability to generalize the training results. The $T$ set is used only once for the final evaluation of the trained ANN.

Stage 4 is the evaluation of the trained network using the selected quality measures. The accuracy of the network predictions was quantified by the root of the mean squared error difference $RMSE$, according to Eq. (11), between the measured $y_i$ and the predicted values $\widehat{y}_i$, the determination coefficient $R^2$, according to Eq. (7), and the relative error $RE$ of the sample, according to Eq. (10), independently for $L$, $V$, and $T$ sets:

$$RMSE = \sqrt{\frac{\sum\limits_{p=1}^{N} \sum\limits_{i=1}^{M} \left(y_i - \widehat{y}_i\right)^2}{NM}}, \tag{11}$$

where $p$ is the number of pattern ($p = 1, \ldots, N$), $i$ is the number of output neurons ($i = 1, \ldots, M$).

## 8. Neural modelling of compactibility parameters

Neural networks were used to obtain models with better prediction quality than the statistical models. These models were to predict the parameters $\rho_{d\,max}$ and *wopt* on the basis of parameters describing the soil grain-size distribution: $C_U$, $D_{10}$, $D_{20}$, $D_{30}$, $D_{40}$, $D_{50}$, $D_{60}$, $D_{70}$, $D_{80}$, and $D_{90}$. MLP neural networks were optimized in the number of input variables and the number of neurons in the hidden layers.

### 8.1. Neural networks with one output

Tests optimizing the ANN architectures were carried out for selected networks with one output variable, $\rho_{d\,max}$ or $w_{opt}$. For modelling the particular parameters ANNs with 10 inputs ($C_U$, $D_{10}$, $D_{20}$, $D_{30}$, $D_{40}$, $D_{50}$, $D_{60}$, $D_{70}$, $D_{80}$, and $D_{90}$), one hidden layer and one output were applied. During optimization of ANN architecture, useless variables (as a result of zero weights) were ignored in some models.

The architecture of the selected best ANNs model for predicting $w_{opt}$ is denoted by 5-4-1 to refer to the number of nodes in the input ($C_U$, $D_{10}$, $D_{20}$, $D_{70}$, $D_{80}$) and in the hidden and output layers, respectively. The topology of the best ANNs model for predicting $\rho_{d\,max}$ is denoted by 10-4-1. Accuracy statistics of the best ANNs with one output are given in Table 3 (see page 29).

### 8.2. ANN with two outputs

For simultaneous modelling of pairs of compactibility parameters, ANNs with one hidden layer and two outputs $\rho_{d\,max}$ and $w_{opt}$ were applied. During optimization of ANN architecture, useless variables (as a result of zero weights) were ignored in some models. The architecture of the selected ANNs model is denoted by 8-9-2. Accuracy statistics of the best ANN with two outputs are presented in Table 3.

### 8.3. Comparison of models

Analysis of the data from Table 3 (especially for the testing set) indicated that: (*i*) all the selected models had sufficiently good prediction quality, (*ii*) quality of the network modelling of the dependence of $w_{opt}$ on five input variables was slightly worse than the network modelling of $\rho_{d\,max}$ dependence on the whole set of ten grain-size distribution characteristics, and (*iii*) qualities of networks with one output $\rho_{d\,max}$ or $w_{opt}$ were comparable to the network that simultaneously modelled these two parameters. Comparisons between the experimental compactibility parameters and those computed by ANN are shown in Figs. 9 to 12. The progress of the training process was moni-
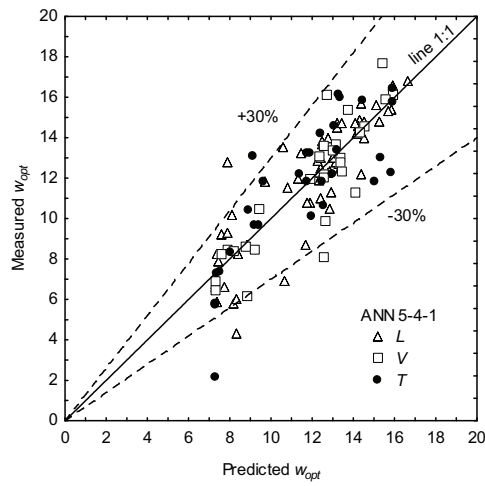
**Fig. 9.** Comparison between experimental values of $w_{\mathrm{opt}}$ and the values calculated by 5-4-1 ANN model, with $\pm 30\%$ $RE$ line
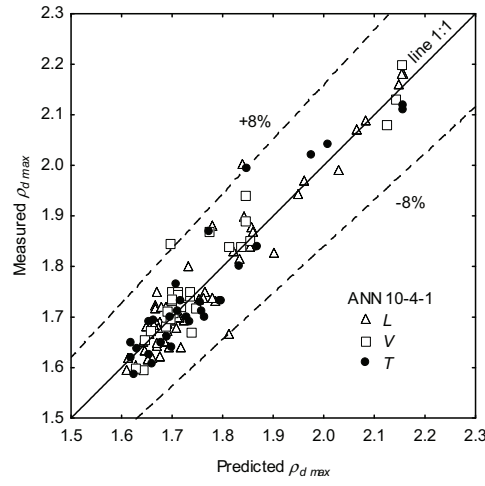


**Fig. 10.** Comparison between experimental values of $\rho_{d\,\max}$ and the values calculated by 10-4-1 ANN model, with $\pm 8\%$ $RE$ line
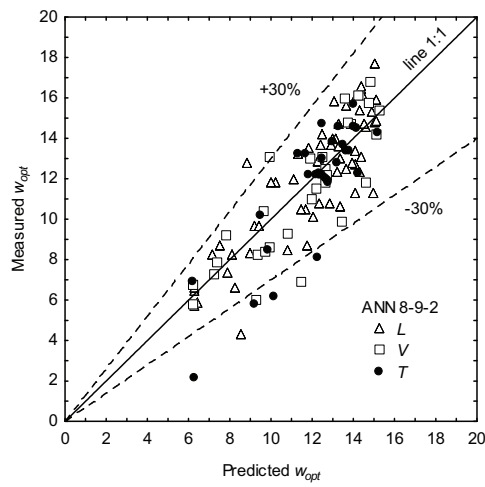


**Fig. 11.** Comparison between experimental values of $w_{\mathrm{opt}}$ and the values calculated by 8-9-2 ANN model, with $\pm 30\%$ $RE$ line
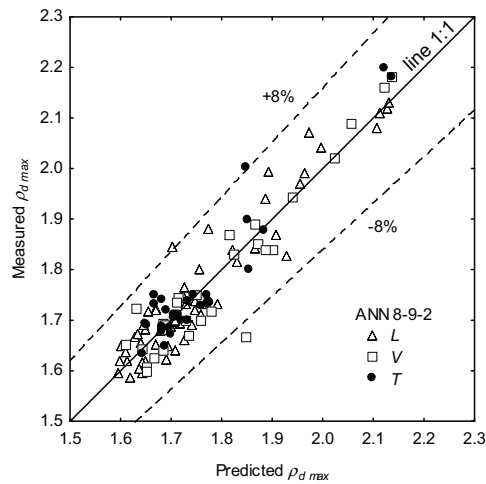
**Fig. 12.** Comparison between experimental values of $\rho_{\text{d max}}$ and the values calculated by 8-9-2 ANN model, with $\pm 8\%$ $RE$ line

tored by observing the $RMSE$ at every iteration of the learning process. Figure 13 represents the variation of error measure during training. Besides, performance of the network during training was also evaluated using the validation patterns, as shown in Fig. 13. During this process it was vital to observe the signs of 'overfitting'. Table 3 shows, after how many epochs the learning process was stopped.

## 9. CONCLUSIONS

Soil compactibility parameters $\rho_{\text{d max}}$ and $w_{\text{opt}}$ are the basic parameters for designing, constructing and controlling the compaction quality of earth structures. Soil compactibility can be determined from a laboratory compactibility curve using Proctor's test. However, this is a destructive, time-consuming and expensive procedure.

In order to more easily determine compactibility parameters of the cohesionless soil, correlations between $\rho_{\text{d max}}$ or $w_{\text{opt}}$ and basic parameters characterizing the soil grain-size distribution were developed. Thus compactibility parameters can be determined by sieve analysis results.

Statistical analysis of the test results of the analyzed soils indicated that: ($i$) soil grain-size distribution significantly influenced $w_{\text{opt}}$ and $\rho_{\text{d max}}$, ($ii$) there were statistically significant linear correlations between $w_{\text{opt}}$ or $\rho_{\text{d max}}$ and grain-size distribution parameters $C_{\text{U}}$, $D_{10}$, $D_{20}$, $D_{30}$, $D_{40}$, $D_{50}$, $D_{60}$, $D_{70}$, $D_{80}$, and $D_{90}$ (with correlation coefficients $r = -0.58$ to $-0.71$ and $r = 0.71$ to 0.88, respectively), ($iii$) linear and nonlinear correlations between $w_{\text{opt}}$ and $C_{\text{U}}$ (with determination coefficients $R^2 = 0.46$ and $R^2 = 0.51$, respectively), and correlations between $\rho_{\text{d max}}$ and $C_{\text{U}}$ (with $R^2 = 0.72$ and $R^2 = 0.73$, respectively) were developed, and ($iv$) statistically significant multiple regression models (with $R^2 = 0.64$ and $R^2 = 0.85$ for $w_{\text{opt}}$ and $\rho_{\text{d max}}$, respectively) were developed.

Artificial neural networks were applied in order to obtain models with better prediction quality. Optimizations of ANNs were performed and the following networks were selected: ($i$) 5-4-1 network modelling $w_{\text{opt}}$ with $R^2 = 0.65$ in testing set, ($ii$) 10-4-1 network modelling $\rho_{\text{d max}}$ with $R^2 = 0.89$ in testing set, and ($iii$) 8-9-2 network modelling simultaneously $w_{\text{opt}}$ or $\rho_{\text{d max}}$ with $R^2 = 0.73$ and 0.89 in testing set, respectively. The neural models had slightly higher prediction accuracy than the statistical models. Relative error of $w_{\text{opt}}$ prediction was about 30% and relative error of $\rho_{\text{d max}}$ prediction was about 8%.

The present study showed that ANNs could analyze regressions in geotechnics and to solve practical engineering problems. The correlations developed can be used for quick determinations of compactibility parameters in cohesionless soils, without performing Proctor's test. Additional test data for different soils can train the ANNs for new soils and make their application more universal.
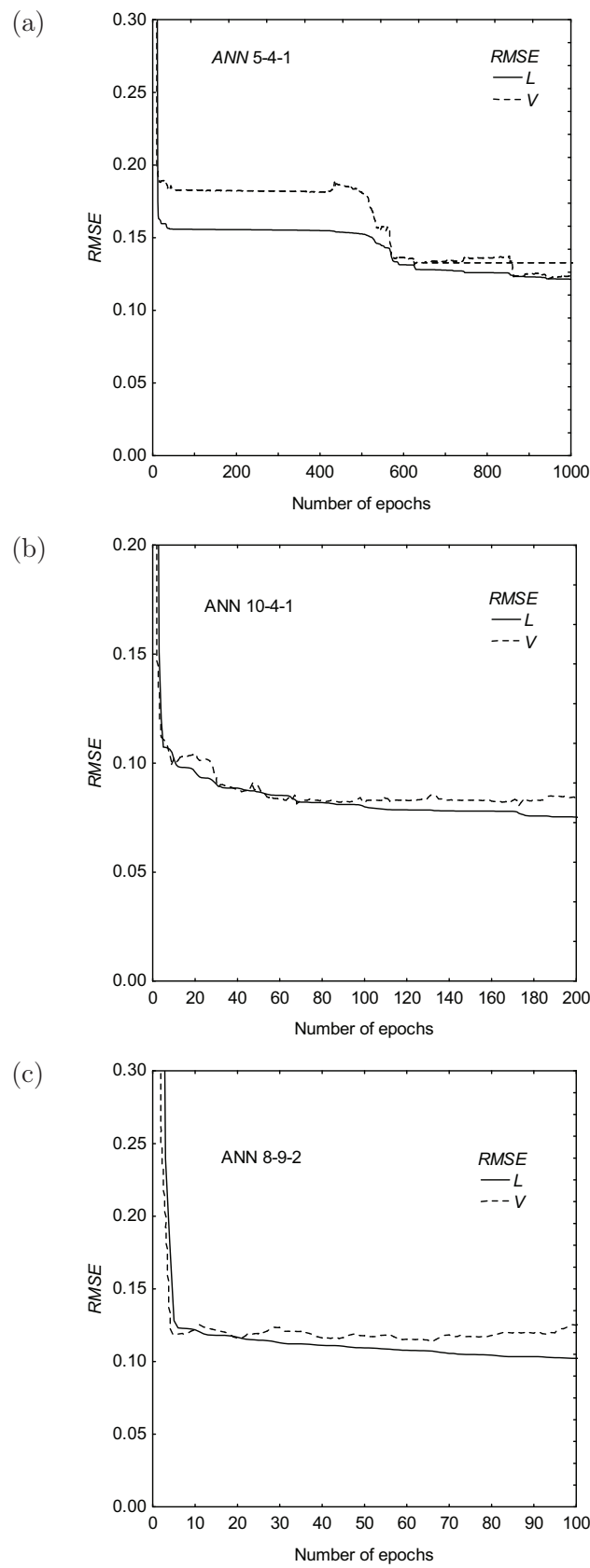
(a)



(b)



(c)



**Fig. 13.** Variation of $RMSE$ with iteration for learning and validation stages for ANNs: (a) 5-4-1, (b) 10-4-1, (c) 8-9-2

## Acknowledgements

## References

[1] I. Håkansson, J. Lipiec. A review of the usefulness of relative bulk density values in studies of soil structure and compaction. *Soil & Tillage Research*, **53**(2): 71–85, 2000.

[2] A.R. Rodriguez, H. Castillo, G.F. Sowers. *Soil mechanics in highway engineering.* Trans Tech Publications, Claustahl-Zellerfeld, 1988.

[3] R.R. Proctor. Fundamental principles of soil compaction. *Engineering News Record*, **111**(9): 245–248, 1993.

[4] R.R. Proctor. Description of field and laboratory methods. *Engineering News Record*, **111**(9): 286–289, 1933.

[5] K.L. Lee, A. Singh. Relative density and relative compaction. *Journal of the Soil Mechanics and Foundations Division*, **97**(SM7): 1049–1052, 1971.

[6] K. Terzaghi. Modern conceptions concerning foundation engineering. *Journal of the Boston Society of Civil Engineers*, **12**(10): 397–439, 1925. Reprinted in: *Contributions to Soil Mechanics 1925–1940*, pp. 1–43, Boston Society of Civil Engineers, Boston, 1940.

[7] L.R. Blotz, C.H. Benson, G.P. Boutwell. Estimating optimum water content and maximum dry unit weight for compacted clays. *Journal of Geotechnical and Geoenvironmental Engineering*, **124**(9): 907–912, 1998.

[8] Y. Gurtug, A. Sridharan. Prediction of compaction characteristics of fine-grained soils. *Géotechnique*, **52**(10): 761–763, 2002.

[9] O. Günaydm. Estimation of soil compaction parameters by using statistical analyses and artificial neural networks. *Environmental Geology*, **57**(1): 203–215, 2009.

[10] Y.M. Najjar, I.A. Basheer, W.A. Naouss. On the identification of compaction characteristics by neuronets. *Computers and Geotechnics*, **18**(3), 167–187, 1996.

[11] S.K. Sinha, M.C. Wang. Artificial neural network prediction models for soil compaction and permeability. *Geotechnical and Geological Engineering*, **26**(1): 47–64, 2008.

[12] I.A. Basheer. Empirical modeling of the compaction curve of cohesive soils. *Canadian Geotechnical Journal*, **38**(1): 29–45, 2001.

[13] U. Lemberg, D.M. Mets. Density? In: D.M. Mets, ed., *Proceedings of the 9th Baltic Geotechnical Conference*, pp.221–225, Tallin, Estonia, 2003.

[14] *STATISTICA System Reference* (Polish edition). StatSoft Polska, Kraków, Polska, 2002.

[15] M.G. Kendall, W.R. Buckland. *A dictionary of statistical terms.* International Statistical Institute by Longman Group Ltd, London-New York, 1982.

[16] M. Evans, N. Hastings, B. Peacock. *Statistical distributions.* Wiley, New York, 1993.

[17] N.R. Draper, H. Smith. *Applied regression analysis.* John Wiley and Sons, New York-London-Sydney, 1966.

[18] R.B. Darlington. *Regression and linear models.* McGraw-Hill, New York, 1990.

[19] R.R. Hocking. *Methods and applications of linear models. Regression and the Analysis of Variance.* Wiley, New York, 1996.

[20] D.M. Bates, D.G. Watts. *Nonlinear regression analysis and its applications.* Wiley, New York, 1984.

[21] T. Masters. *Practical neural network recipes in C++.* Academic Press, New York, 1993.

[22] S. Haykin. *Neural networks: A comprehensive foundation.* Macmillan Publishing, New York, 1994.

[23] Z. Waszczyszyn, ed. *Neural networks in the analysis and design of structures.* CISM Courses and Lectures, **404**, Springer, Wien-New York, 1999.

[24] K. Hornik. Approximation capabilities of multilayer feedforward network. *Neural Networks*, **4**(2): 251-257, 1991.

[25] L.V. Fausett. *Fundamentals neural networks: architecture, algorithms, and applications.* Prentice-Hall, New Jersey, 1994.

[26] *STATISTICA Neural Networks* (Polish edition). StatSoft Polska, Kraków, Polska, 2001.

[27] P. Gill, W. CityMurray, M. Wright. *Practical optimization.* Academic Press, New York, 1981.

[28] W.H. Press, S.A. Teukolsky, W.T. Vetterling, B.P. Flannery. *Numerical recipes. The art of scientific computing.* Cambridge University Press, Cambridge, 2007.